SCHOLIX RESEARCH SIMPLIFIED

International Surgery and Case Reports

Open access

High-Fidelity-Guided Surrogate Optimization of Compartment Fire Dynamics Using Trust-Region Model Management

Volume 1, Issue 3, Article 1

Date of Submission : 25-08-2026

Date of Acceptance : 30-08-2026

Date of Publication : 11-09-2026

Lakshmi. N. Sridhar

Chemical Engineering Department

University of Puerto Rico

Mayaguez, PR 00681

***Corresponding author**: Lakshmi. N. Sridhar.

Abstract

High-fidelity computational fire simulations provide detailed information on transient compartment-fire behavior but can become computationally expensive when repeatedly evaluated for parametric analysis and optimization. This study develops an integrated framework combining the Fire Dynamics Simulator (FDS), artificial neural-network surrogate modeling, and trust-region model management for compartment-fire analysis and ventilation optimization. High-fidelity FDS simulations were performed to investigate the effects of fire intensity and doorway width on transient gas temperatures measured at three elevations within a ventilated compartment. The resulting transient dataset was used to train a neural-network surrogate with heat-release rate per unit area, doorway width, and time as inputs. The surrogate was subsequently incorporated into a trust-region model-management framework in which candidate solutions were evaluated against additional high-fidelity FDS simulations. Although the initial surrogate achieved an overall coefficient of determination of approximately 0.71 for the held-out ventilation case, local discrepancies between surrogate and FDS predictions produced incorrect optimization trends, demonstrating that satisfactory overall predictive accuracy does not necessarily ensure optimization reliability. Additional high-fidelity evaluations and adaptive surrogate refinement improved portions of the local response but did not completely eliminate errors in peak-temperature magnitude, timing, and local trend. Within the high-fidelity-supported interval of doorway widths from 0.800 to 1.000 m, the lowest evaluated peak lower-level temperature was 1090 °C at 0.800 m, approximately 1.8% below the value at 1.000 m. A three-mesh grid-sensitivity assessment further showed that absolute temperature predictions remained dependent on spatial resolution. The results demonstrate the importance of high-fidelity verification and local model management when data-driven surrogates are used for optimization of transient fire-dynamics systems.

Keywords: Fire Dynamics Simulator (FDS); Compartment Fire; Neural-Network Surrogate Modeling; Trust-Region Model Management; Ventilation Optimization

Introduction

Compartment fires are governed by strongly coupled interactions among heat release, buoyancy-driven flow, turbulent mixing, heat transfer, and ventilation. Among these factors, ventilation plays a particularly important role because the size and configuration of openings control the supply of oxygen to the fire and the transport of hot gases from the enclosure. Changes in doorway or window geometry can therefore alter burning behavior, gas temperatures, flow patterns, and the transition between well-ventilated and under-ventilated fire regimes. These interactions are inherently transient and nonlinear, making computational modeling an important tool for systematically investigating compartment-fire behavior.

Computational fluid dynamics (CFD) has become widely used for resolving the spatial and temporal development of fire-driven flows. The Fire Dynamics Simulator (FDS), developed by the National Institute of Standards and Technology, solves a form of the Navier–Stokes equations appropriate for low-speed, thermally driven flows, with particular emphasis on smoke and heat transport from fires [1]. Its large-eddy-simulation formulation enables detailed investigation of quantities such as gas temperature, velocity, species transport, and heat transfer and has made FDS an established computational platform for fire research and engineering applications [1,2].

Ventilation effects in compartment fires have received considerable attention because opening geometry can fundamentally alter the available combustion regimes. Lafdal et al. [3] performed more than 300 FDS simulations of naturally ventilated compartment fires with different enclosure scales, opening heights and widths, and heat-release rates. Their analysis identified well-ventilated, transitional, and under-ventilated regimes and demonstrated the strong relationship between opening characteristics, ventilation, and the resulting thermal response. More recently, Beshir et al. [4] combined full-scale experiments and numerical modeling to examine the effects of ventilation position, opening area, and opening aspect ratio on compartment-fire dynamics. Their results further demonstrated that changes in opening configuration influence internal fire behavior, heat fluxes, and the conditions associated with flashover. Collectively, these studies show that ventilation cannot always be represented by a simple monotonic relationship between opening size and a single thermal response variable.

Although high-fidelity CFD provides detailed information about compartment-fire dynamics, repeated simulations can become computationally expensive when many combinations of operating and geometric parameters must be investigated. This limitation becomes particularly important when the high-fidelity model is embedded within an optimization procedure, because the simulator may need to be evaluated repeatedly as the optimizer explores the design space. Surrogate modeling provides an attractive alternative by learning an approximate relationship between simulation inputs and outputs from a finite set of high-fidelity calculations and subsequently evaluating that relationship at substantially lower computational cost.

Machine-learning methods have consequently attracted increasing interest as surrogate models for computationally demanding fire simulations. Nguyen et al. [5], for example, developed machine-learning surrogate models for calibration of fire-source properties in FDS simulations of façade-fire tests. Their study considered both multiple linear regression and artificial neural networks and demonstrated that surrogate models could be coupled with optimization while selected solutions were subsequently verified using FDS. This work illustrates the potential of data-driven models to reduce the number of direct high-fidelity evaluations required in fire-engineering applications. Neural networks are particularly attractive for transient surrogate modeling because they can represent nonlinear mappings between multiple operating variables, time, and system responses.

The use of a surrogate within an optimization algorithm, however, introduces an additional challenge. Good predictive performance over a training or validation dataset does not necessarily imply that the surrogate will reproduce the local behavior of the high-fidelity model in the region explored by the optimizer. Small local errors may change the predicted direction of improvement, and an optimizer may exploit inaccuracies in the surrogate rather than identify genuine improvement in the underlying high-fidelity system. Consequently, surrogate-assisted optimization requires a mechanism for controlling the region in which the surrogate is trusted and for verifying candidate solutions against the original high-fidelity model.

Trust-region model-management methods provide a systematic framework for addressing this problem. Eason and Biegler [6] developed a trust-region filter approach for optimization problems containing computationally expensive black-box components represented by reduced models. Subsequent work extended the strategy and demonstrated its application to hybrid glass-box/black-box optimization problems [7]. More recently, Biegler [8] reviewed the trust-region filter strategy for optimization with surrogate models and emphasized the combination of computationally inexpensive surrogate optimization with intermittent evaluation of the high-fidelity truth model. Related recent developments have continued to investigate more efficient reduced-model construction and sampling strategies for computationally expensive black-box optimization [9]. These approaches provide an important conceptual basis for combining inexpensive surrogate calculations with selective high-fidelity evaluations rather than relying on the surrogate throughout the optimization process.

Despite advances in both computational fire modeling and surrogate-based optimization, comparatively limited attention has been directed toward integrating transient FDS simulations, neural-network surrogate modeling, adaptive high-fidelity evaluation, and trust-region model management specifically for compartment-fire ventilation optimization. Previous fire studies have demonstrated the importance of ventilation and the usefulness of FDS for resolving compartment-fire behavior [3,4], while machine-learning studies have demonstrated the feasibility of replacing repeated FDS evaluations with computationally efficient surrogate models for calibration and related tasks [5]. Trust-region methods, meanwhile, provide a rigorous foundation for managing discrepancies between surrogate and high-fidelity models [6–9]. Bringing these elements together provides an opportunity to examine not only whether a surrogate can approximate fire simulations, but also whether its local predictions are sufficiently reliable to support optimization decisions.

In this study, we develop an integrated computational framework combining high-fidelity FDS simulations, neural-network surrogate modeling, and trust-region model management for transient compartment-fire analysis and ventilation optimization. High-fidelity simulations are first used to investigate the effects of fire intensity and doorway width on temperatures measured at multiple elevations within a ventilated compartment. The complete transient temperature histories are then used to construct and evaluate a neural-network surrogate with heat-release rate per unit area, doorway width, and simulation time as inputs. Doorway width is subsequently treated as the design variable in a surrogate-assisted optimization framework, while additional FDS simulations are used to evaluate proposed candidates, quantify local surrogate discrepancies, and guide adaptive surrogate refinement. A grid-sensitivity assessment using three progressively refined computational meshes is also performed to characterize the numerical-resolution dependence of the predicted temperatures.

The principal contribution of this work is the integration of transient fire simulation, data-driven surrogate modeling, and high-fidelity-guided trust-region model management within a unified computational workflow. Rather than assuming that a surrogate with acceptable overall predictive performance remains reliable during optimization, the framework explicitly evaluates local agreement between surrogate and FDS predictions before accepting optimization-driven conclusions. The resulting analysis therefore provides both an assessment of the potential of neural-network surrogates for reducing the computational burden of fire-dynamics optimization and a demonstration of the importance of high-fidelity model management when localized surrogate errors influence the predicted direction of improvement.

METHODOLOGY

Computational Framework

We developed a computational framework to investigate transient fire dynamics in a ventilated compartment and provide high-fidelity simulation data for subsequent reduced-order modeling and trust-region optimization. We used Fire Dynamics Simulator (FDS), Version 6.11.1, as the high-fidelity computational model. FDS is based on a large-eddy simulation formulation for low-speed, thermally driven flows and is particularly suited to simulating heat and smoke transport associated with fires. We used Smokeview to visualize the transient temperature fields generated by FDS.

We implemented the overall computational framework in stages. First, we established a baseline compartment-fire model in FDS. We then used parametric simulations to characterize the system response to variations in fire intensity and ventilation. We used the resulting high-fidelity transient data to construct a computationally inexpensive neural-network surrogate model. The surrogate and FDS models were subsequently incorporated into a trust-region model-management framework in which the surrogate generated candidate solutions and FDS served as the high-fidelity reference model.

Compartment Geometry and Computational Domain

A rectangular compartment having the following dimensions was considered $3.0\,\mathrm{m} \times 3.0\,\mathrm{m} \times 2.4\,\mathrm{m}$ The computational domain was discretized using a structured mesh containing $30 \times 30 \times 24$ computational cells. This corresponds to a nominal uniform grid spacing of approximately $\Delta x = \Delta y = \Delta z = 0.10\,\mathrm{m}$. The compartment consisted of a floor, ceiling, side walls, back wall, and front wall containing a doorway. The baseline doorway width was $W_{\mathrm{door}} = 0.8\mathrm{m}$ and the doorway height was $H_{\mathrm{door}} = 2.0\mathrm{m}$. The baseline computational domain was discretized using a structured mesh of 30 × 30 × 24 cells, corresponding to a nominal grid spacing of approximately 0.10 m. A grid-sensitivity assessment was subsequently performed using two progressively finer meshes of 40 × 40 × 32 and 50 × 50 × 40 cells, corresponding to nominal grid spacings of approximately 0.075 and 0.060 m, respectively. The results of this assessment are presented and discussed below.

Fire Source

Propane was selected as the fuel for the initial compartment-fire simulations. The fire source was positioned near the center of the compartment and occupied a horizontal area of $0.5\,\mathrm{m} \times 0.5\,\mathrm{m}$ The fire intensity was specified in FDS through the heat release rate per unit area (HRRPUA). The baseline simulation employed $\mathrm{HRRPUA} = 400\mathrm{kW/m^2}$.Each simulation was conducted for a total physical time of $t_f = 60\mathrm{s}$

Temperature Monitoring

Gas temperatures were monitored at three vertical positions near the compartment center. The measurement locations were designated TEMP_LOW, TEMP_MID, and TEMP_HIGH. Their respective vertical positions were: $z_{\mathrm{low}} = 0.5\mathrm{m}, z_{\mathrm{mid}} = 1.2,\mathrm{m} z_{\mathrm{high}} = 2.0\mathrm{m}.$ These locations were selected to characterize the transient thermal response at different elevations within the compartment. FDS automatically recorded temperature histories and exported them through the device-output CSV files.In addition to the point measurements, a vertical temperature slice through the center of the computational domain was generated at $x = 1.5\,\mathrm{m}$. The temperature slice was visualized in Smokeview and represented the transient spatial development of the thermal field within the compartment.

Baseline Simulation

An initial simulation was performed using the baseline fire intensity $\mathrm{HRRPUA} = 400\mathrm{kW/m^2}$. The FDS calculation completed successfully, and Smokeview visualized the resulting temperature field. The transient temperature histories measured at the three monitoring locations were subsequently extracted from the FDS device-output file. The temperature signals exhibited substantial temporal fluctuations associated with the transient and turbulent nature of the compartment-fire flow. These data provide the initial high-fidelity response against which subsequent parametric simulations can be compared.

Fire-Intensity Parametric Study

After successfully executing the baseline model, a preliminary parametric investigation examined the sensitivity of the compartment thermal response to fire intensity. Five values of HRRPUA were considered $\mathrm{HRRPUA} = 200, 300, 400, 500, 600\mathrm{kW/m^2}$. All other model parameters, including compartment dimensions, mesh resolution, doorway geometry, fire location, sensor positions, and simulation duration, were maintained unchanged. This one-factor-at-a-time approach isolated the effect of fire intensity. We generated separate FDS input files for each fire-intensity condition, and all five simulations completed successfully. We obtained temperature-versus-time histories from the corresponding device-output files.We extracted the maximum temperature measured at the TEMP_LOW location as an initial scalar measure of the thermal response. If the transient temperature at this location is represented by $T_{\mathrm{low}}(t)$, the maximum temperature over the simulation interval was defined $T_{\mathrm{low,max}} = \max_{0 \le t \le t_f} T_{\mathrm{low}}(t)$ where the final simulation time was: $t_f = 60\mathrm{s}$ .The maximum temperatures measured at the lower monitoring location are summarized in Table 1.

HRRPUA (kW/ m²)	Maximum TEMP_LOW (°C)
200	754.88
300	approximately 985
400	approximately 1090
500	approximately 1180
600	approximately 1220

Table 1. Maximum gas temperature at the lower monitoring location for different imposed fire intensities.

The simulations demonstrate an overall increase in maximum gas temperature with increasing HRRPUA. The investigated fire-intensity range was $200\mathrm{kW/m^2} \le \mathrm{HRRPUA} \le 600\mathrm{kW/m^2}$ Across this range, the observed maximum TEMP_LOW value increased from approximately: $T_{\mathrm{low,max}} = 755^{\circ}\mathrm{C}$ to approximately: $T_{\mathrm{low,max}} = 1220^{\circ}\mathrm{C}$. The incremental temperature increase became smaller toward the upper end of the investigated HRRPUA range, suggesting that the relationship between the imposed fire intensity and the local maximum temperature is nonlinear.

The instantaneous temperature histories also exhibited pronounced fluctuations. Such fluctuations are expected in transient fire-driven flows because the measurement location is influenced by the evolving buoyant plume and turbulent transport. Consequently, subsequent analysis will consider not only instantaneous maximum temperatures but also appropriate time-averaged and statistical measures of the thermal response. These results characterize the comparative response of the consistently discretized FDS model to changes in fire intensity. As discussed in the grid-sensitivity assessment below, the absolute temperature predictions remain sensitive to mesh resolution; consequently, emphasis is placed on comparative trends among simulations performed using the same computational mesh.

Transition to Ventilation and Surrogate Modeling

The initial FDS model and fire-intensity parametric study established the high-fidelity computational foundation for the subsequent optimization framework. We next investigated the influence of ventilation by systematically varying the doorway width while maintaining the fire intensity and remaining model parameters constant. The baseline doorway width was 0.8 m, and we maintained the fire intensity at an HRRPUA of 400 kW/m². The ventilation study was particularly important to the optimization framework because doorway width subsequently served as the design variable. The resulting high-fidelity dataset was subsequently used to construct a neural-network surrogate representation of the transient fire dynamics. Let the ventilation control variable be denoted by u. The surrogate model can then be represented generally as:

$$\hat{\mathbf{y}} = M_{\mathrm{ROM}}(u) \quad 1$$

where: $\hat{\mathbf{y}}$ represents the predicted quantities of interest, such as compartment temperatures.
The subsequent optimization problem sought a doorway width that minimized the selected fire-safety objective. In general, this may be represented as:

$$\min_u J(u) \quad 2$$

subject to the relevant physical, operational, and fire-safety constraints.In the Biegler-type trust-region framework, optimization of the computationally inexpensive surrogate model will be restricted locally around the current iterate u_k.
The trust-region constraint is written as:

$$\|u - u_k\| \le \Delta_k \quad 3$$

where Δ_k denotes the trust-region radius at iteration k.
Candidate solutions generated using the surrogate model were evaluated using the high-fidelity FDS model. Agreement between the surrogate prediction and the FDS response was used to determine whether a candidate step was accepted and whether the trust-region radius should be increased or decreased. This model-management strategy combined the computational efficiency of surrogate-based optimization with the reliability of high-fidelity fire-dynamics simulations.

Results

Ventilation Parametric Study

Following the fire-intensity parametric study, a second set of simulations was initiated to investigate ventilation's influence on the compartment thermal response. The doorway width was selected as the ventilation parameter, while the fire intensity was maintained constant at $\mathrm{HRRPUA} = 400, \mathrm{kW/m^2}$. The baseline doorway width was $W_{\mathrm{door}} = 0.8, \mathrm{m}$. To investigate the effect of reduced ventilation, the doorway width was decreased to $W_{\mathrm{door}} = 0.4, \mathrm{m}$, while the doorway height, compartment geometry, computational mesh, fire location, sensor locations, and simulation duration were maintained unchanged. The doorway remained centered at the same location on the front wall so that doorway width was the principal geometric parameter varied in this simulation. The FDS simulation for the $W_{\mathrm{door}} = 0.4, \mathrm{m}$ case completed successfully. We extracted the temperature history at the TEMP_LOW monitoring location from the corresponding FDS device-output file. The preliminary maximum temperature was approximately $T_{\mathrm{low,max}} = 1150,^{\circ}\mathrm{C}$. For comparison, the baseline $W_{\mathrm{door}} = 0.8, \mathrm{m}$ case at the same fire intensity produced a maximum TEMP_LOW value of approximately $1090,^{\circ}\mathrm{C}$. Thus, the initial calculation indicates that reducing the doorway width increased the maximum local temperature under the conditions investigated. Additional doorway widths were subsequently simulated to characterize the relationship between ventilation and compartment temperature over the investigated range. The subsequent simulation with a doorway width of $W_{\mathrm{door}} = 0.6, \mathrm{m}$ produced a maximum temperature of approximately $T_{\mathrm{low,max}} = 1120,^{\circ}\mathrm{C}$, providing an additional intermediate ventilation condition between the $0.4, \mathrm{m}$ and baseline $0.8, \mathrm{m}$ doorway cases. The simulation with a doorway width of $W_{\mathrm{door}} = 1.0, \mathrm{m}$ produced a maximum temperature of approximately $T_{\mathrm{low,max}} = 1110,^{\circ}\mathrm{C}$. This value was slightly higher than that obtained for the baseline $0.8, \mathrm{m}$ doorway, indicating that the relationship between doorway width and the instantaneous maximum local temperature may not be strictly monotonic. The final simulation in the initial ventilation series used a doorway width of $W_{\mathrm{door}} = 1.2, \mathrm{m}$. The resulting maximum temperature was approximately $T_{\mathrm{low,max}} = 1110,^{\circ}\mathrm{C}$. Considering the complete set of doorway-width simulations, the maximum TEMP_LOW decreased from approximately $1150,^{\circ}\mathrm{C}$ at $W_{\mathrm{door}} = 0.4, \mathrm{m}$ to approximately $1090,^{\circ}\mathrm{C}$ at the baseline width of $W_{\mathrm{door}} = 0.8, \mathrm{m}$, followed by values of approximately $1110,^{\circ}\mathrm{C}$ for both the $1.0, \mathrm{m}$ and $1.2, \mathrm{m}$ cases. These results indicate a non-monotonic dependence of the instantaneous maximum local temperature on doorway width. We therefore retained the complete transient temperature histories for subsequent surrogate-model development rather than relying exclusively on a single maximum-temperature measure. Figure 1 illustrates this non-monotonic dependence of peak TEMP_LOW on doorway width, with the lowest value among the initial ventilation cases occurring at the 0.800 m doorway width. Table 2 shows the effect of doorway width on maximum TEMP_LOW at HRRPUA = 400 kW/m².

Doorway width (m)	HRRPUA (kW/m²)	Maximum TEMP_LOW (°C)
0.4	400	≈1150
0.6	400	≈1120
0.8	400	≈1090
1.0	400	≈1110
1.2	**400**	**≈1110**

Table 2. Effect of doorway width on maximum TEMP_LOW at HRRPUA = 400 kW/m².

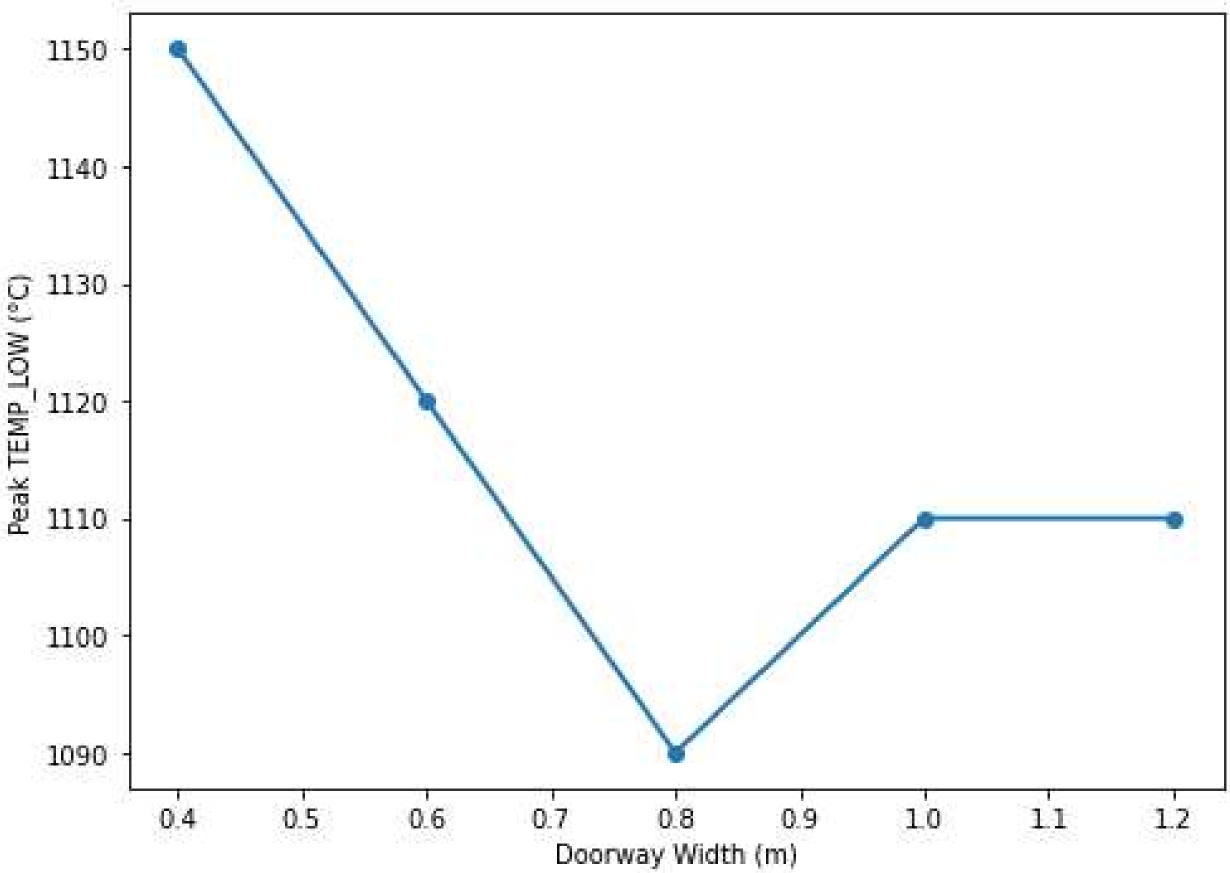

Fig. 1. Effect of doorway width on the peak TEMP_LOW obtained from the high-fidelity FDS simulations at an HRRPUA of 400 kW/m².

Grid-Sensitivity Assessment

A grid-sensitivity assessment was performed for the baseline condition of HRRPUA = 400 kW/m² and a doorway width of 0.8 m. Three structured meshes were evaluated: 30 × 30 × 24, 40 × 40 × 32, and 50 × 50 × 40 cells, corresponding to nominal grid spacings of approximately 0.10, 0.075, and 0.060 m, respectively. All other model parameters, geometry, sensor locations, and simulation conditions were maintained unchanged so that the effect of spatial resolution could be assessed directly.

Table 3 summarizes the effect of computational mesh refinement on the maximum temperatures predicted at the three monitoring locations for the baseline condition.

Table 3. Grid-sensitivity assessment for the baseline condition at HRRPUA = 400 kW/m² and doorway width = 0.8 m.

Mesh	Grid spacing (m)	Max TEMP_LOW (°C)	Max TEMP_MID (°C)	Max TEMP_HIGH (°C)
30 × 30 × 24	0.100	1090	753	499
40 × 40 × 32	0.075	1120	900	641
50 × 50 × 40	0.060	1220	1130	702

The grid-sensitivity results indicate that the predicted temperatures remained dependent on spatial resolution over the range of meshes investigated. Refinement from a nominal grid spacing of 0.10 m to 0.075 m increased the maximum temperatures at all three monitoring locations, and further refinement to 0.060 m produced additional increases. The changes were particularly pronounced for TEMP_LOW and TEMP_MID, whereas the difference in TEMP_HIGH

became smaller between the two finer meshes. These results indicate that complete grid convergence was not achieved within the investigated mesh range. Accordingly, the absolute temperature values obtained using the baseline mesh should be interpreted with appropriate numerical-resolution uncertainty.

Because the parametric, surrogate-modeling, and model-management calculations were developed from simulations performed using the same 30 × 30 × 24 baseline mesh, comparisons among those cases were made on a consistent numerical basis. The grid-sensitivity results nevertheless indicate that the reported absolute temperatures should not be interpreted as mesh-independent predictions. The present analysis therefore focuses primarily on comparative trends among consistently simulated cases and on the performance of the surrogate/model-management framework, while further mesh refinement remains appropriate for applications requiring grid-converged absolute temperature predictions.

High-Fidelity Dataset Preparation for Surrogate Modeling

Following completion of the fire-intensity and ventilation parametric simulations, the FDS outputs were organized into a unified high-fidelity dataset for subsequent surrogate-model development. Two input parameters were considered: the imposed fire intensity, represented by HRRPUA, and the doorway width, represented by W_{door}. The thermal response was characterized using the maximum temperatures measured at the three monitoring locations TEMP_LOW, TEMP_MID, and TEMP_HIGH. These response quantities are denoted by $T_{\mathrm{low,max}}$, $T_{\mathrm{mid,max}}$, and $T_{\mathrm{high,max}}$, respectively. For each temperature signal, the maximum value over the simulation interval was calculated according to:

$$T_{j,\max} = \max_{0 \le t \le t_f} T_j(t) \tag{4}$$

where j represents the LOW, MID, or HIGH monitoring location and $t_f = 60,\mathrm{s}$ is the final simulation time. A master dataset was constructed containing the simulation case, HRRPUA, doorway width, maximum temperatures at the three monitoring locations, and the corresponding FDS device-output file. The resulting high-fidelity dataset is summarized in Table 4.

Table 4. High-fidelity FDS dataset prepared for surrogate-model development

Case	HRRPUA (kW/m²)	Door width (m)	Max TEMP_LOW (°C)	Max TEMP_MID (°C)	Max TEMP_HIGH (°C)
Fire_200	200	0.8	754.88	501	327
Fire_300	300	0.8	985	613	394
Fire_400	400	0.8	1090	753	499
Fire_500	500	0.8	1180	914	602
Fire_600	600	0.8	1220	1050	684
Vent_04	400	0.4	1150	765	513
Vent_06	400	0.6	1120	793	544
Vent_10	400	1.0	1110	785	500
Vent_12	400	1.2	1110	838	545

The assembled dataset demonstrates that increasing fire intensity produces a clear increase in the maximum temperature at all three monitoring elevations. In contrast, variation of doorway width produces a more complex response that differs among the three monitoring locations. These results indicate that a surrogate representation based exclusively on a single maximum temperature may not adequately characterize the compartment thermal response. Accordingly, the

three temperature measurements were retained as response variables, and the underlying transient temperature histories were used for surrogate-model development.

Transient Data Preparation for Surrogate Modeling

Following preparation of the summary high-fidelity dataset, the transient FDS temperature data were organized for subsequent surrogate-model development. Complete time histories of TEMP_LOW, TEMP_MID, and TEMP_HIGH were extracted from the FDS device-output files for all nine unique simulation cases considered in the fire-intensity and ventilation studies. These cases include five fire-intensity conditions with $\mathrm{HRRPUA} = 200, 300, 400, 500,$ and $600,\mathrm{kW/m^2}$ at the baseline doorway width of $W_{\mathrm{door}} = 0.8,\mathrm{m}$, together with the ventilation cases $W_{\mathrm{door}} = 0.4, 0.6, 1.0,$ and $1.2,\mathrm{m}$ at $\mathrm{HRRPUA} = 400,\mathrm{kW/m^2}$. The baseline $400,\mathrm{kW/m^2}$, $0.8,\mathrm{m}$ case is common to both parameter studies and was therefore retained as a single unique simulation. For each case, simulation time and the three corresponding temperature histories were incorporated into the master dataset.

For each simulation case, the transient dataset therefore consists of the time-dependent response vector

$$\mathbf{T}(t) = \left[T_{\mathrm{low}}(t),, T_{\mathrm{mid}}(t),, T_{\mathrm{high}}(t) \right]^T \quad 5$$

over the FDS simulation interval. Retaining the complete temperature histories, rather than only their maximum values, preserves information concerning the temporal evolution and fluctuations of the compartment thermal field. These transient data were subsequently processed and used to construct and evaluate the neural-network surrogate representation of the high-fidelity FDS model.

<u>Combined Transient Dataset</u>

To facilitate subsequent surrogate-model development, the transient data from the nine unique FDS simulations were assembled into a single combined dataset. Each observation contains the imposed fire intensity (HRRPUA), doorway width, simulation time, and the corresponding TEMP_LOW, TEMP_MID, and TEMP_HIGH values. The resulting dataset therefore provides a unified mapping from the operating conditions and simulation time to the transient thermal response. This organization enabled systematic preprocessing, surrogate-model training, and subsequent evaluation against the high-fidelity FDS simulations.

Data Preprocessing

Before surrogate-model development, the combined transient dataset underwent a structural quality check to verify continuity of the simulation variables and correct alignment of the nine FDS cases. We assigned each observation a case identifier and established a case-based training and testing partition. The Vent_10 case, corresponding to a doorway width of 1.0 m at an HRRPUA of 400 kW/m², was withheld as an independent test case, while the remaining eight cases were assigned to the training dataset. We scaled the surrogate-model inputs—HRRPUA, doorway width, and simulation time—before model development. HRRPUA was scaled over the investigated range of 200–600 kW/m², doorway width over 0.4–1.2 m, and simulation time over 0–60 s. We also scaled the three temperature responses, TEMP_LOW, TEMP_MID, and TEMP_HIGH, to facilitate numerical training. This preprocessing provided a consistent dataset for surrogate-model development and evaluation at an operating condition excluded from model training.

Surrogate Model Development and Validation

We developed a feed-forward artificial neural network as a computationally efficient surrogate for the high-fidelity FDS simulations. The surrogate uses scaled fire intensity (HRRPUA), doorway width, and simulation time as inputs and predicts transient temperatures at the three monitoring locations: TEMP_LOW, TEMP_MID, and TEMP_HIGH. We used a multilayer perceptron architecture with the rectified linear unit (ReLU) activation function. We examined several

network configurations and selected a four-hidden-layer architecture with 150, 150, 100, and 50 neurons, respectively, for subsequent analysis.
We used a case-based validation strategy rather than randomly splitting individual transient observations. The Vent_10 case, corresponding to HRRPUA = 400 kW/m² and a doorway width of 1.0 m, was excluded from model training and used as an independent test condition. The remaining eight simulation cases were used to train the surrogate. For the held-out Vent_10 case, the surrogate produced R^2 values of 0.724, 0.771, and 0.626 for TEMP_LOW, TEMP_MID, and TEMP_HIGH, respectively. The corresponding root-mean-square errors were 113.7 °C, 83.3 °C, and 52.8 °C, while the mean absolute errors were 74.4 °C, 67.1 °C, and 42.7 °C, respectively. The overall R^2 across the three temperature responses was 0.707.

Comparison of the predicted and FDS temperature histories showed that the surrogate captures the principal transient heating and cooling behavior but does not reproduce all of the short-timescale fluctuations present in the high-fidelity FDS signals. A diagnostic comparison against smoothed FDS temperature histories produced substantially higher coefficients of determination, indicating that a considerable component of the prediction error is associated with these rapid fluctuations rather than the underlying transient thermal trend. Nevertheless, we retained the raw FDS histories as the primary basis for model validation.

We also examined the sensitivity of the neural-network solution to random initialization using five random seeds. The overall test score ranged from approximately 0.619 to 0.707, with a mean of approximately 0.656. We retained a fixed random seed of 42 to ensure reproducibility for the subsequent optimization calculations. The trained surrogate was then stored independently and successfully reloaded and evaluated within a separate optimization framework. This enables rapid prediction of the transient thermal response at candidate operating conditions without repeatedly retraining the neural network.

Trust-Region Optimization Framework

The validated surrogate model was subsequently incorporated into a trust-region optimization framework based on the model-management principles described by Biegler[8], in which the computationally inexpensive surrogate is used to generate candidate solutions within a local trust region and the high-fidelity FDS model is used to assess the reliability of those candidates. The doorway width was treated as the design variable while the fire intensity was fixed at an HRRPUA of $400 \text{ kW} / \text{m}^2$. The optimization objective was defined as the maximum value of the predicted lower-level temperature, TEMP_LOW, over the 60-s fire simulation,

$$J\left(W_{\text{door}}\right) = \max_{0 \le t \le 60} T_{\text{LOW}}\left(t; W_{\text{door}}\right) \qquad 6$$

The allowable doorway width was bounded between 0.4 and 1.2 m. We evaluated the transient surrogate response using 101 uniformly spaced time points between 0 and 60 s. An initial trust-region center of $W_{\text{door}} = 1.0 \text{ m}$ and an initial trust-region radius of $\Delta = 0.2 \text{ m}$ were selected, resulting in an initial local search interval of $0.8 \le W_{\text{door}} \le 1.2 \text{ m}$. Within this initial trust region, the surrogate-based optimization subproblem was solved to identify a candidate doorway width that reduced the predicted maximum TEMP_LOW. At the initial center, the surrogate predicted a maximum TEMP_LOW of 974.70°C. The first surrogate subproblem proposed a candidate doorway width of approximately 0.967 m, for which the predicted maximum TEMP_LOW was 973.02°C, corresponding to a predicted reduction of approximately 1.69°C. The surrogate-generated candidate is not accepted solely on the basis of the reduced-order prediction. Instead, the candidate operating condition is evaluated using the high-fidelity FDS model. The resulting high-fidelity objective value is then compared with the surrogate-predicted improvement to determine whether to accept the candidate and

whether to expand, maintain, or reduce the trust-region radius. This iterative surrogate/high-fidelity comparison underpins control of the optimization procedure's reliability.

We then evaluated the first surrogate-generated candidate using the high-fidelity FDS model. At the current trust-region center of $W_{\text{door}} = 1.0\text{m}$, the high-fidelity FDS objective was 1110.00°C. At the surrogate-proposed candidate of $W_{\text{door}} \approx 0.967\text{m}$, FDS produced a maximum TEMP_LOW of 1115.17°C. Thus, although the surrogate predicted a reduction in the objective from 974.70°C to 973.02°C, the corresponding high-fidelity calculation showed an increase of 5.17°C. The agreement ratio between the actual and predicted objective reductions was calculated as

$$\rho = \frac{J_{\text{FDS}}(1.0) - J_{\text{FDS}}(0.967)}{J_{\text{sur}}(1.0) - J_{\text{sur}}(0.967)}. \quad 7$$

Using the calculated objective values, the agreement ratio was approximately $\rho = -3.07$. The negative value of ρ indicates disagreement between the surrogate and high-fidelity models regarding the direction of improvement. Consistent with trust-region model-management principles, disagreement between the surrogate and high-fidelity model provides a basis for rejecting the candidate and contracting the trust region to improve local surrogate reliability [8].Consequently, the first candidate was rejected and the trust-region center was retained at $W_{\text{door}} = 1.0\text{m}$. The trust-region radius was subsequently reduced before solving the next local surrogate subproblem.
Following rejection of the first candidate, the trust-region radius was progressively contracted while retaining the current center at $W_{\text{door}} = 1.0$ m. Radii of 0.10 and 0.05 m continued to produce essentially the same surrogate optimum near $W_{\text{door}} = 0.967$ m and therefore did not require redundant high-fidelity evaluations. Further contraction to $\Delta = 0.025$ m restricted the local search interval to $0.975 \le W_{\text{door}} \le 1.025$ m and produced a new candidate of $W_{\text{door}} = 0.975$ m. The surrogate predicted an objective of 973.048°C, corresponding to a predicted reduction of 1.657°C relative to the current center. High-fidelity FDS evaluation, however, yielded a maximum lower-level temperature of 1115.786°C, compared with 1110.00°C at the current center. The resulting actual reduction was therefore -5.786°C, giving an agreement ratio of approximately $\rho = -3.49$. The candidate was consequently rejected and the trust-region center remained at $W_{\text{door}} = 1.0$ m. The repeated disagreement between the surrogate-predicted and FDS-observed directions of improvement indicates that additional local model management is required before proceeding with further trust-region steps.

Local Model-Management Assessment.

The need for this local model-management assessment is consistent with Biegler [8], who emphasized that surrogate accuracy over a training dataset alone does not ensure that surrogate-based optimization will reproduce the behavior or optimum of the high-fidelity truth model. After rejecting the trust-region candidates, we used the high-fidelity FDS results to quantify the local discrepancy between the neural-network surrogate and the FDS model. At door widths of 0.967 and 0.975 m, the maximum TEMP_LOW values predicted by the surrogate were 973.03 and 973.07 °C, respectively, compared with corresponding FDS values of 1115.17 and 1115.79 °C. At the current trust-region center of 1.000 m, the surrogate predicted 974.72 °C compared with the FDS value of 1110.00 °C. The corresponding local surrogate discrepancies were therefore approximately 142.14, 142.72, and 135.28 °C. These results demonstrate a systematic local underprediction of the high-fidelity temperature response by the surrogate. We then performed a

preliminary discrepancy-correction analysis using the available high-fidelity points. Although an interpolating local correction reproduced the sampled high-fidelity values, extrapolation outside the sampled region produced behavior that was not sufficiently supported by the available FDS data. Therefore, we did not accept an additional trust-region candidate based on the corrected model at this stage. Instead, we incorporated the high-fidelity evaluations into the subsequent local model-management and surrogate-refinement procedure.

Local Surrogate Refinement

In trust-region model management, additional high-fidelity evaluations can be used to improve the local representation of the surrogate in regions where model disagreement is observed (Biegler[8]). After the local model-management assessment, we incorporated two new high-fidelity FDS trajectories corresponding to doorway widths of 0.967 and 0.975 m into a separate refinement of the neural-network surrogate. The original training dataset contained 8,008 transient observations from eight FDS cases, and the two new high-fidelity simulations added 2,002 observations, resulting in 10,010 observations for surrogate refinement. We retained the Vent_10 case at a doorway width of 1.0 m outside the refinement-training dataset for comparison. The refined surrogate used the same four-hidden-layer architecture containing 150, 150, 100, and 50 neurons with ReLU activation as the original model.

For the Vent_10 case, the refined surrogate produced R^2 values of 0.748, 0.784, and 0.585 for TEMP_LOW, TEMP_MID, and TEMP_HIGH, respectively. The corresponding RMSE values were 108.6 °C, 81.1 °C, and 55.7 °C. Compared with the original surrogate, for which the corresponding RMSE values were 113.7 °C, 83.3 °C, and 52.8 °C, the refinement improved the prediction of TEMP_LOW and TEMP_MID, while TEMP_HIGH showed a modest decrease in predictive accuracy.

The refinement also improved the local prediction errors for the two high-fidelity trust-region cases. For TEMP_LOW, the RMSE decreased from 184.5 to 127.7 °C for the 0.967 m case and from 115.9 to 108.8 °C for the 0.975 m case. However, the refinement did not fully resolve the peak-temperature discrepancy. At a doorway width of 0.967 m, FDS produced a peak TEMP_LOW of 1115.17 °C at 32.76 s, whereas the refined surrogate predicted a peak of 988.20 °C at 29.89 s. At 0.975 m, the FDS peak was 1115.79 °C at 41.89 s, while the refined surrogate predicted 988.49 °C at 29.94 s. At the 1.0 m Vent_10 condition, the corresponding FDS and refined-surrogate peak temperatures were 1110.00 °C and 989.62 °C, respectively.

Thus, although incorporating the new high-fidelity data improved overall local surrogate accuracy, the refined model continued to underpredict peak TEMP_LOW by approximately 120–127 °C and did not reproduce the local non-monotonic variation of the FDS peak temperature with doorway width. Consequently, we retained this first refined surrogate for model-management analysis rather than using it directly to generate another trust-region candidate. These findings motivated additional high-fidelity sampling and further local surrogate refinement, as described in the following sections.

Local Peak-Objective Model Management

To further assess the local reliability of the refined surrogate, we compared the variation of the peak TEMP_LOW objective with doorway width against the available high-fidelity FDS results. Over the interval from 0.967 to 0.975 m, the refined surrogate produced a finite-difference slope of 37.09 °C/m, compared with 77.14 °C/m from FDS. Thus, both models predicted the same direction of variation over this interval. However, over the interval from 0.975 to 1.000 m, the refined surrogate predicted a positive slope of 45.45 °C/m, whereas FDS produced a slope of −231.43 °C/m. The refined surrogate therefore failed to reproduce the reversal in the local high-fidelity peak-temperature response near the current trust-region center.

We subsequently defined the local peak-temperature discrepancy as the difference between the FDS and refined-surrogate peak TEMP_LOW values. The discrepancies at doorway widths of 0.967, 0.975, and 1.000 m were 126.97, 127.29, and 120.37 °C, respectively. A piecewise linear discrepancy correction was applied only within the high-fidelity sampled interval of 0.967–1.000 m, without extrapolation beyond this region. The corrected local model reproduced the three available FDS peak-temperature values and indicated that the minimum within this sampled interval remained at the current trust-region center of 1.000 m, where the FDS peak TEMP_LOW was 1110.00 °C. Consequently, within the locally sampled interval of 0.967–1.000 m, the model-management analysis provided no high-fidelity-supported basis for moving the trust-region iterate toward smaller doorway widths. No additional FDS evaluation was therefore initiated from this corrected local model.

Additional High-Fidelity Evaluation at 0.900 m

The local model-management analysis was extended by performing an additional high-fidelity FDS simulation at a doorway width of 0.900 m. This condition was selected to add a high-fidelity point within the previously sparsely sampled interval between 0.800 and 0.967 m. At an HRRPUA of 400 kW/m², the FDS simulation produced a maximum TEMP_LOW of 1105.694 °C at approximately 33.1 s. The refined surrogate predicted a corresponding peak temperature of 987.975 °C, resulting in a peak-temperature discrepancy of 117.719 °C. The new high-fidelity result provided additional information on the variation of the peak-temperature objective within the previously sparsely sampled interval between 0.800 and 0.967 m. The FDS peak TEMP_LOW increased from approximately 1090 °C at 0.800 m to 1105.694 °C at 0.900 m and 1115.169 °C at 0.967 m. Thus, the additional FDS evaluation confirms an increasing high-fidelity peak-temperature trend over this interval. In contrast, the refined surrogate does not reproduce this trend accurately, further demonstrating that surrogate predictions alone are not yet sufficiently reliable for selecting subsequent trust-region steps. This behavior reinforces the role of the high-fidelity model in trust-region model management, where surrogate-based optimization is coupled with truth-model evaluations to assess and improve the reliability of candidate solutions [8]. We then incorporated the new high-fidelity point into the local model-management and surrogate-refinement procedure to assess whether adaptive high-fidelity enrichment improves the surrogate representation of the peak-temperature objective. A second refined surrogate was trained using the original training data together with high-fidelity trajectories at doorway widths of 0.900, 0.967, and 0.975 m. The updated training set contained 11,011 transient observations. At 0.900 m, the updated surrogate predicted a peak TEMP_LOW of 977.16 °C compared with the FDS value of 1105.694 °C. Although the absolute peak remained underpredicted, the updated surrogate substantially improved the local peak-temperature trend between 0.900 and 0.967 m. Over this interval, the surrogate slope increased from approximately 3.30 °C/m before the additional refinement to 126.83 °C/m after refinement, compared with the corresponding FDS slope of 141.41 °C/m. Despite the improved representation of the local trend, substantial discrepancies between the surrogate and FDS peak-temperature magnitudes remained.

A piecewise-linear high-fidelity discrepancy correction was therefore applied to the updated surrogate using the available FDS evaluations at doorway widths of 0.800, 0.900, 0.967, 0.975, and 1.000 m. By construction, the piecewise-linear correction reproduced the FDS peak temperatures at these high-fidelity support points. Within the supported interval of 0.800–1.000 m, the minimum corrected peak TEMP_LOW occurred at a doorway width of 0.800 m, corresponding to 1090 °C. This result is interpreted as the best model-managed solution within the evaluated interval rather than as a global optimum. Figure 2 compares the high-fidelity FDS peak temperatures with those predicted by the second refined surrogate (v2), illustrating the persistent underprediction of the peak-temperature magnitude and the need for high-fidelity discrepancy correction in the model-management procedure.

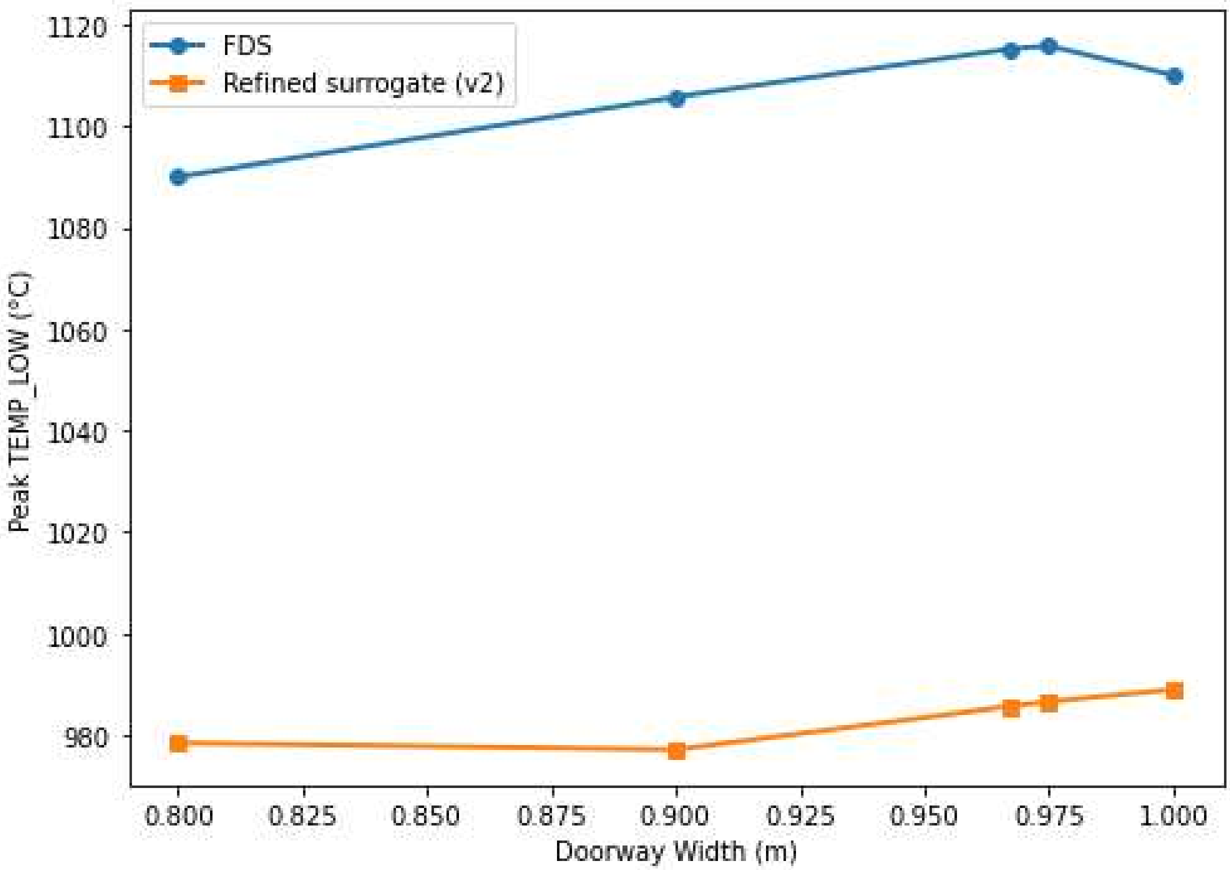

Fig. 2. Comparison of the peak TEMP_LOW predicted by the high-fidelity FDS simulations and the refined surrogate model (v2) as a function of doorway width.

DISCUSSION

The results demonstrate the importance of combining surrogate modeling with high-fidelity verification when optimizing transient compartment-fire dynamics. Although the neural-network surrogate provided a computationally efficient representation of the FDS simulations, discrepancies remained in both the magnitude and local trend of the peak-temperature objective. In particular, surrogate-predicted improvements at some doorway widths were not confirmed by the corresponding FDS simulations. These findings show that surrogate accuracy measured over a broader dataset does not necessarily guarantee sufficient local accuracy in the region explored by the optimization algorithm. The trust-region model-management framework therefore provided an important mechanism for identifying disagreement between the surrogate and high-fidelity models before accepting candidate solutions.

The high-fidelity simulations also revealed a non-monotonic relationship between doorway width and peak compartment temperature. At an HRRPUA of 400 kW/m², the peak TEMP_LOW decreased as the doorway width increased from 0.4 to 0.8 m, with the lowest value among the original ventilation cases occurring at 0.8 m. Further increases in doorway width did not produce an additional reduction in the peak temperature. This behavior indicates that the thermal response cannot be represented adequately by assuming a simple monotonic relationship between ventilation and peak temperature. The result also highlights the value of evaluating the ventilation parameter over multiple high-fidelity simulations rather than inferring an optimum from a limited local trend.

The adaptive refinement results further illustrate the distinction between improving surrogate accuracy and achieving optimization-relevant fidelity. Incorporating the additional high-fidelity trajectories improved the surrogate representation in portions of the locally sampled region, particularly the predicted trend between doorway widths of 0.900 and 0.967 m. However, substantial errors remained in the predicted peak-temperature magnitude, and the refined surrogate still failed to reproduce the high-fidelity trend between 0.800 and 0.900 m. Thus, additional training data improved aspects of the local surrogate response but did not uniformly resolve the model discrepancy. These results support the continued use of high-fidelity verification when surrogate predictions are used to guide optimization decisions.

Within the high-fidelity-supported interval of 0.800–1.000 m, the model-management analysis identified a doorway width of 0.800 m as the best evaluated solution, with a peak TEMP_LOW of 1090 °C. This value represents a reduction of approximately 1.8% relative to the 1110 °C peak obtained at the initial 1.000 m doorway width. Importantly, this result should not be interpreted as a global optimum. Rather, it represents the best solution supported by the available high-fidelity evaluations and the local model-management analysis. This distinction is important because the surrogate model exhibited significant discrepancies in the optimization region, making extrapolation beyond the high-fidelity-supported interval inappropriate.

More broadly, the results demonstrate the value of model management for fire-dynamics optimization when high-fidelity simulations are computationally expensive and surrogate predictions contain localized errors. The surrogate can rapidly explore the design space, while selected FDS evaluations provide high-fidelity information needed to assess candidate solutions and identify regions where the surrogate requires refinement. The present study therefore illustrates a practical coupling of transient fire simulation, neural-network surrogate modeling, and trust-region model management. At the same time, the observed surrogate–FDS discrepancies emphasize that high-fidelity evaluations remain essential when optimization decisions depend on relatively small differences in the predicted objective.

Several limitations should be considered when interpreting these results. The optimization was conducted over a limited range of doorway widths and used peak TEMP_LOW over the 60-s simulation period as the primary objective. The surrogate model also exhibited residual errors in both peak magnitude and timing despite adaptive refinement. The grid-sensitivity assessment further showed that the absolute temperature predictions remained dependent on spatial resolution over the investigated mesh range, with complete grid convergence not achieved. Accordingly, the quantitative temperature values should be interpreted with numerical-resolution uncertainty, while comparisons among the parametric and optimization cases remain based on a consistent baseline mesh.In addition, the present implementation adopts trust-region model-management principles in a simplified objective-based form rather than implementing the complete trust-region filter algorithm. Consequently, the results should be interpreted as demonstrating the feasibility and value of high-fidelity-guided surrogate optimization for the present compartment-fire problem rather than establishing a global optimum or a universally applicable fire-control strategy.

CONCLUSIONS

This study developed a computational framework that integrates high-fidelity FDS simulations, neural-network surrogate modeling, and trust-region model management for the analysis and optimization of transient compartment-fire dynamics. Parametric FDS simulations characterized the effects of fire intensity and doorway width on compartment temperatures, and the resulting transient data were used to train and evaluate the surrogate model. The surrogate was then incorporated into an iterative model-management procedure in which candidate solutions were assessed against additional high-fidelity FDS simulations. This approach enabled discrepancies between surrogate predictions and the high-fidelity response to be identified explicitly during the optimization process.

For the ventilation conditions investigated at an HRRPUA of 400 kW/m², the high-fidelity simulations showed a non-monotonic dependence of peak TEMP_LOW on doorway width. Within the high-fidelity-supported interval of 0.800–1.000 m, the model-management analysis identified 0.800 m as the best evaluated doorway width, corresponding to a peak TEMP_LOW of 1090 °C. This represents an approximately 1.8% reduction relative to the 1110 °C peak at the initial 1.000 m doorway width. The result is interpreted as the best model-managed solution within the evaluated interval and not as a global optimum.

The results demonstrate that surrogate accuracy alone is insufficient for reliable optimization when localized discrepancies occur between the surrogate and high-fidelity model. Additional FDS evaluations and adaptive surrogate refinement improved the representation of portions of the local response but did not eliminate errors in peak-temperature magnitude and trend. High-fidelity verification therefore remained essential for evaluating optimization candidates. The grid-sensitivity assessment also demonstrated that the absolute temperature predictions remained dependent on mesh resolution, emphasizing the need to distinguish comparative trends obtained on a consistent mesh from grid-converged quantitative temperature predictions. The framework developed in this study provides a foundation for future work involving broader ventilation and fire conditions, improved adaptive surrogate models, and more complete trust-region filter formulations for computational fire-safety optimization.

ACKNOWLEDGEMENT

The author thanks Dr. Biegler for teaching him the trust-region strategy. The author thanks Dr. Carlos Ramirez for encouraging him to write single author papers.

REFERENCES

1. McGrattan, K. B., McDermott, R., Weinschenk, C., Overholt, K., Hostikka, S., and Floyd, J. (2013). *Fire Dynamics Simulator Technical Reference Guide, Volume 1: Mathematical Model*, Sixth Edition. NIST Special Publication 1018, National Institute of Standards and Technology. https://doi.org/10.6028/NIST.SP.1018e6.
2. McGrattan, K. B., McDermott, R., Weinschenk, C., and Forney, G. P. (2013). *Fire Dynamics Simulator User's Guide*, Sixth Edition. NIST Special Publication 1019, National Institute of Standards and Technology. https://doi.org/10.6028/NIST.SP.1019.
3. Lafdal, B., Djebbar, R., Boulet, P., Mehaddi, R., Koutaiba, E. M., Beji, T., and Torero, J. L. (2022). Numerical study of the combustion regimes in naturally-vented compartment fires. *Fire Safety Journal*, 131, 103604. https://doi.org/10.1016/j.firesaf.2022.103604.
4. Beshir, M., Wang, Y., Cicione, A., Krajcovic, M., Hadden, R., and Rush, D. (2025). Qualitative analysis of ventilation position and dimension effects on compartment fire dynamics: An experimental and numerical approach. *Fire Technology*, 61, 3615–3647. https://doi.org/10.1007/s10694-025-01747-5.
5. Nguyen, H. T., Abu-Zidan, Y., Zhang, G., and Nguyen, K. T. Q. (2022). Machine learning-based surrogate model for calibrating fire source properties in FDS models of façade fire tests. *Fire Safety Journal*, 130, 103591. https://doi.org/10.1016/j.firesaf.2022.103591.
6. Eason, J. P., and Biegler, L. T. (2016). A trust region filter method for glass box/black box optimization. *AIChE Journal*, 62(9), 3124–3136. https://doi.org/10.1002/aic.15325.

7. Eason, J. P., and Biegler, L. T. (2018). Advanced trust region optimization strategies for glass box/black box models. *AIChE Journal*, 64, 3934–3943. https://doi.org/10.1002/aic.16364.
8. Biegler, L. T. (2024). The trust region filter strategy: Survey of a rigorous approach for optimization with surrogate models. *Digital Chemical Engineering*, 13, 100197. https://doi.org/10.1016/j.dche.2024.100197.
9. Liang, R., Han, Y., Hu, H., Chen, B., Yuan, Z., and Biegler, L. T. (2024). Efficient trust region filter modeling strategies for computationally expensive black-box optimization. *Computers & Chemical Engineering*, 189, 108816. https://doi.org/10.1016/j.compchemeng.2024.108816.